Supporting Information for

"*In-vitro* Replication Studies on O^2-Methylthymidine and O^4-Methylthymidine"

Nisana Andersen[1], Jianshuang Wang[1], Pengcheng Wang[2], Yong Jiang[2] and Yinsheng Wang[1,2,*]

[1]Department of Chemistry and [2]Environmental Toxicology Graduate Program, University of California, Riverside, California 92521-0403

Chem. Res. Toxicol., 2012

Figure S1. Product-ion spectrum of the $[M-4H]^{4-}$ ion (*m/z* 1300.4) of the 17-mer ODN d(CCATGGCA*X*GAGAATTC), where "*X*" is O^2-MdT (A) and O^4-MdT (B). Shown in the inset is the negative-ion ESI-MS for the ODNs.

Figure S2. Calibration curves for the ratios of unextended primer d(AATTCTC) to d(AATTCTCATGC) (i.e., 11A) (A); d(AATTCTCA) (i.e., 8A) to 11A (B); d(AATTCTCG) (i.e., 8G) to 11A (C); d(AATTCTCTGC) (i.e., 10Del) to 11A (D); d(AATTCTCCTGC) (i.e., 11C) to 11A (E); d(AATTCTCTTGC) (i.e., 11T) to 11A (F); d(AATTCTCGTGC) (i.e., 11G) to 11A (G).

Figure S3. Representative gel images for steady-state kinetic assays measuring nucleotide incorporation opposite undamaged dT (A), O^2-MdT (B), and O^4-MdT (C) with Kf^- (0.7-7 nM). Reactions were conducted in the presence of individual dNTPs with the highest concentrations indicated in the figures. The ratios of dNTP concentrations were 0.5-0.6 between neighboring lanes.

Figure S4. Representative gel images for steady-state kinetic assays measuring nucleotide incorporation opposite undamaged dT (A), O^2-MdT (B), and O^4-MdT (C) with human DNA polymerase κ (1-5 nM). Reactions were conducted in the presence of individual dNTPs with the highest concentrations indicated in the figures. The concentration ratios of dNTP between neighboring lanes were 0.5-0.6.

Figure S5. Representative gel images for steady-state kinetic assays measuring nucleotide incorporation opposite undamaged dT (A), O^2-MdT (B), and O^4-MdT (C) with yeast polymerase η (7.5 nM). Reactions were conducted in the presence of individual dNTPs with the highest concentrations indicated in the figures. The concentration ratios of dNTP between neighboring lanes were 0.5-0.6.

Figure S6. (A) The total-ion chromatogram derived from the LC-MS/MS analysis of the human pol κ-induced replication products of O^2-MdT-containing substrates that have been treated with two restriction enzymes, NcoI and EcoRI plus shrimp alkaline phosphatase. (B) ESI-MS averaged from the peaks eluting in 18.5-20.5 min in part (A), where 'T*' designates the remnant of the digested template containing the damaged site, i.e., d(CATGGCA*X*GAG), where '*X*' is O^2-MdT, and 'P*' designates the 5' portion of the digested primer, i.e., d(GCTAGGATCATAG)

Figure S7. Analysis of the unextended primer and +1 extension products from the human pol κ-induced replication reaction arising from replication of O^2-MdT-containing substrates that have been treated with two restriction enzymes, NcoI and EcoRI, and shrimp alkaline phosphatase. Product-ion spectra of the ESI-produced $[M-2H]^{2-}$ ion of: the 7mer, d(AATTCTC) (precursor ion *m/z* 1026.2) (A); 8A, d(AATTCTCA) (precursor ion *m/z* 1182.7) (B); 8G, d(AATTCTCG) (precursor ion *m/z* 1190.7) (C); 10Del, d(AATTCTCTGC) (precursor ion *m/z* 1487.3) (D). In this and the following MS/MS figures, the arrow indicates the fragmentation process, and the solid and open circles represent the precursor ion and fragment ions, respectively.

Figure S8. Analysis of full-length extension products from the human pol κ-induced replication reaction arising from replication of O^2-MdT-containing substrates that have been treated with

two restriction enzymes, NcoI and EcoRI, and shrimp alkaline phosphatase. Product-ion spectra of the ESI-produced $[M-2H]^{2-}$ ions of: 11C, d(AATTCTCCTGC) (precursor ion *m/z* 1631.8) (A); 11T, d(AATTCTCTTGC) (precursor ion *m/z* 1639.3) (B); 11A, d(AATTCTCATGC) (precursor ion *m/z* 1643.8) (C); 11G, d(AATTCTCGTGC) (precursor ion *m/z* 1651.7) (D).

Figure S9. The selected-ion chromatograms (SICs) derived from the LC-MS/MS analysis of the replication mixture of the substrate containing dT with: Klenow fragment exo$^-$ (A), yeast pol η (B), and human pol κ (C).

Figure S10. The SICs derived from the LC-MS/MS analysis of the replication mixture of the substrate containing O^2-MdT with: Klenow fragment exo$^-$ (A), and yeast pol η (B).

Figure S11. The SICs derived from the LC-MS/MS analysis of the replication mixture of the substrate containing O^4-MdT with: Klenow fragment exo$^-$ (A), yeast pol η (B), and human pol κ (C).

Figure S12. LC-MS/MS for monitoring possible demethylation of O^2-MdT-containing template following primer extension with human pol κ and restriction digestion. Shown are the SICs derived from ultra-zoom scans monitoring the $[M-3H]^{3-}$ ions from the unmethylated and O^2-MdT 12mer arising from the digestion of the original O^2-MdT-containing template.

Figure S13. LC-MS/MS for monitoring possible demethylation of O^2-MdT-containing templates following primer extension with human pol κ. Shown are the product-ion spectra of the ESI-produced $[M-3H]^{3-}$ ions of: unmethylated 12mer, d(CATGGCCA**T**GAG) (precursor ion *m/z* 1221.9) (A); original 12mer, d(CATGGCCA[***O*^{2}-MdT**]GAG) (precursor ion *m/z* 1226.5) (B).

Figure S14. The SICs derived from the LC-MS/MS analysis of the replication mixture of the substrate containing O^4-MdT with yeast pol η: low dNTPs (A), 6 hr (B).

Figure S15. Representative gel images for steady-state kinetic assays measuring extension past undamaged dT (A), O^2-MdT (B), and O^4-MdT (C) with the base opposite the lesion indicated in the figure. Reactions were conducted with human polymerase κ (1-5 nM) in the presence of individual dNTPs with the highest concentrations indicated in the figures. The concentration ratios of dNTP between neighboring lanes were 0.5-0.6.

Table S1. Summary of the percentages of replication products produced for O^4-MdT-containing substrates by yeast pol η as determined by LC-ESI-MS/MS experiments. Reactions were conducted under two separate conditions: (1) low dNTPs concentrations (50 μM each) at 37°C overnight; (2) 1 mM dNTPs at 37°C for 6 hr. The template was d(CCATGGCA***X***GAGAATTCTATGATCCTAG), where ***'X'*** represents O^4-MdT.

Table S2. Efficiency and fidelity of human polymerase κ-mediated nucleotide extension with dATP and dGTP opposite undamaged dT, O^2-MdT and O^4-MdT as determined by steady-state kinetic measurements.

(A)

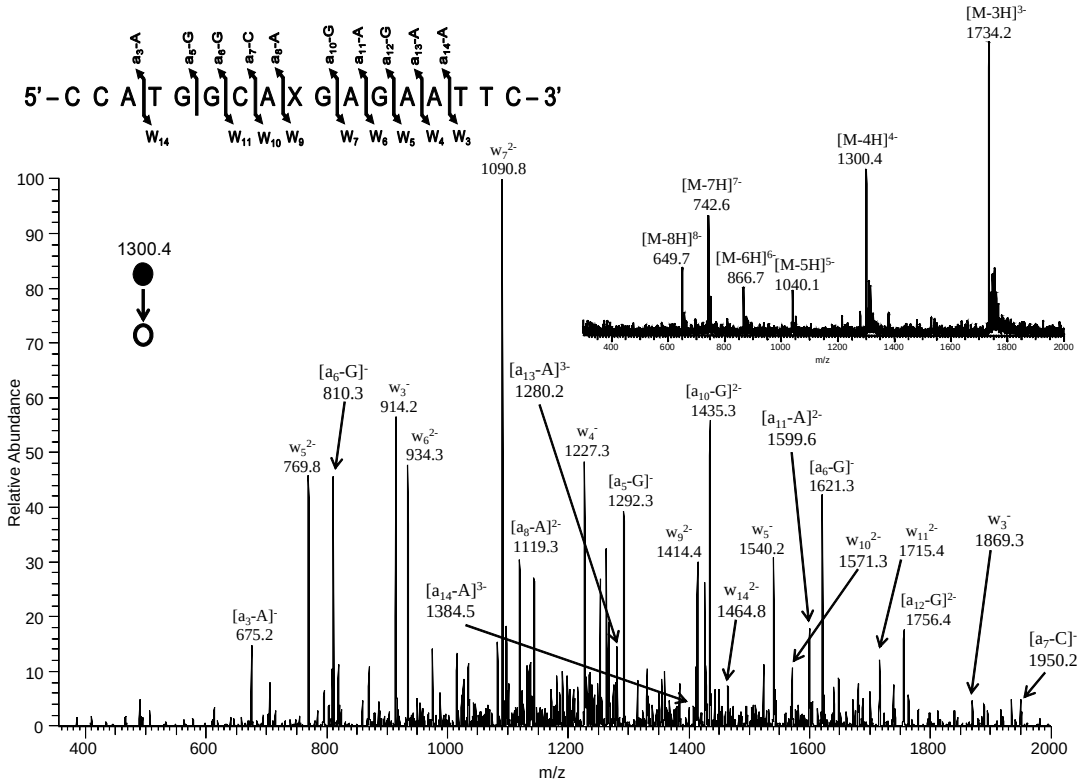
5'-C C A T G G C A X G A G A A T T C-3'
a3-A a5-G a6-G a7-C a8-A a10-G a11-A a12-G a13-A a14-A
W14 W11 W10 W9 W7 W6 W5 W4 W3
1300.4
[M-3H]3- 1734.2
[M-4H]4- 1300.4
[M-7H]7- 742.6
[M-8H]8- 649.7
[M-6H]6- 866.7
[M-5H]5- 1040.1
w7 2- 1090.8
[a6-G]- 810.3
w3 - 914.2
w5 2- 769.8
w6 2- 934.3
[a13-A]3- 1280.2
w4 - 1227.3
[a5-G]- 1292.3
[a10-G]2- 1435.3
[a11-A]2- 1599.6
[a6-G]- 1621.3
[a8-A]2- 1119.3
w9 2- 1414.4
w5 - 1540.2
w10 2- 1571.3
w11 2- 1715.4
w3 - 1869.3
[a14-A]3- 1384.5
w14 2- 1464.8
[a12-G]2- 1756.4
[a3-A]- 675.2
[a7-C]- 1950.2
Relative Abundance
m/z

(B)

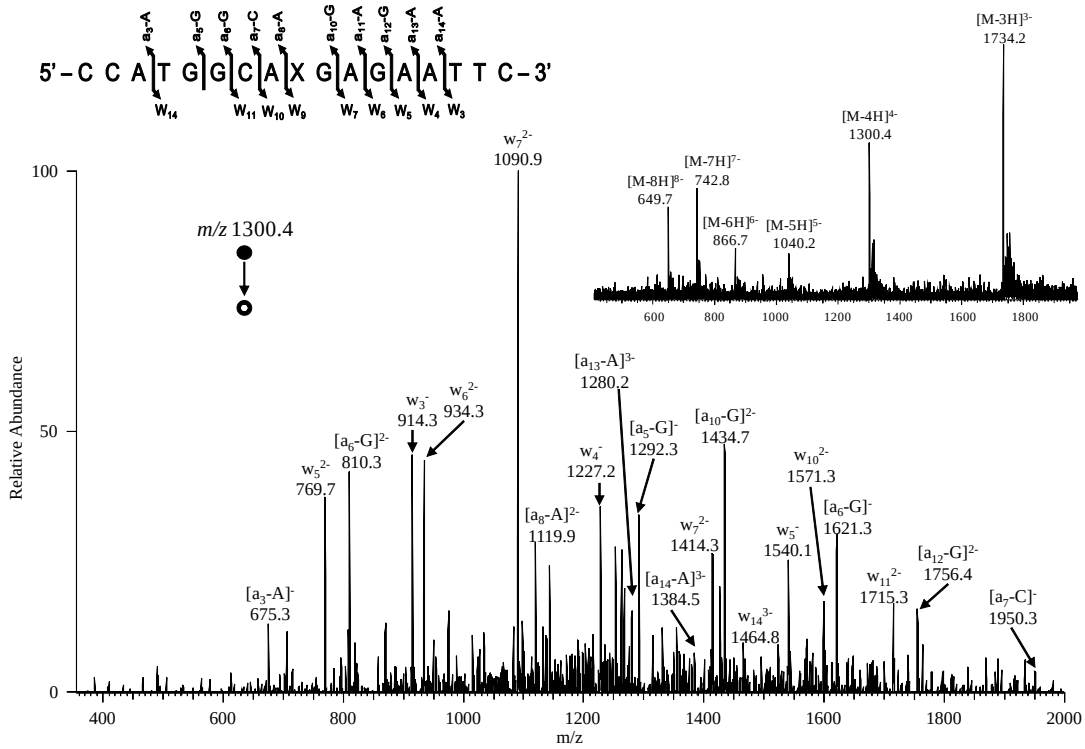
5'-C C A T G G C A X G A G A A T T C-3'
a3-A a5-G a6-G a7-C a8-A a10-G a11-A a12-G a13-A a14-A
W14 W11 W10 W9 W7 W6 W5 W4 W3
m/z 1300.4
[M-3H]3- 1734.2
[M-4H]4- 1300.4
[M-7H]7- 742.8
[M-8H]8- 649.7
[M-6H]6- 866.7
[M-5H]5- 1040.2
w7 2- 1090.9
[a13-A]3- 1280.2
w3 - 914.3
w6 2- 934.3
[a6-G]2- 810.3
w5 2- 769.7
[a5-G]- 1292.3
[a10-G]2- 1434.7
w4 - 1227.2
w10 2- 1571.3
[a6-G]- 1621.3
[a8-A]2- 1119.9
w7 2- 1414.3
w5 - 1540.1
[a12-G]2- 1756.4
w11 2- 1715.3
[a14-A]3- 1384.5
[a3-A]- 675.3
w14 3- 1464.8
[a7-C]- 1950.3
Relative Abundance
m/z

Figure S1.

(A)

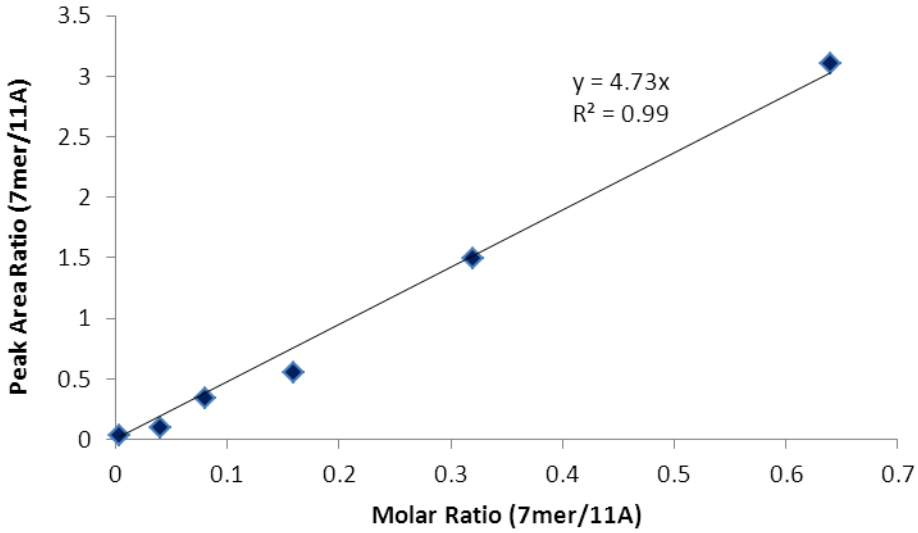
y = 4.73x
R² = 0.99
Peak Area Ratio (7mer/11A)
Molar Ratio (7mer/11A)
0
0.5
1
1.5
2
2.5
3
3.5
0
0.1
0.2
0.3
0.4
0.5
0.6
0.7

(B)

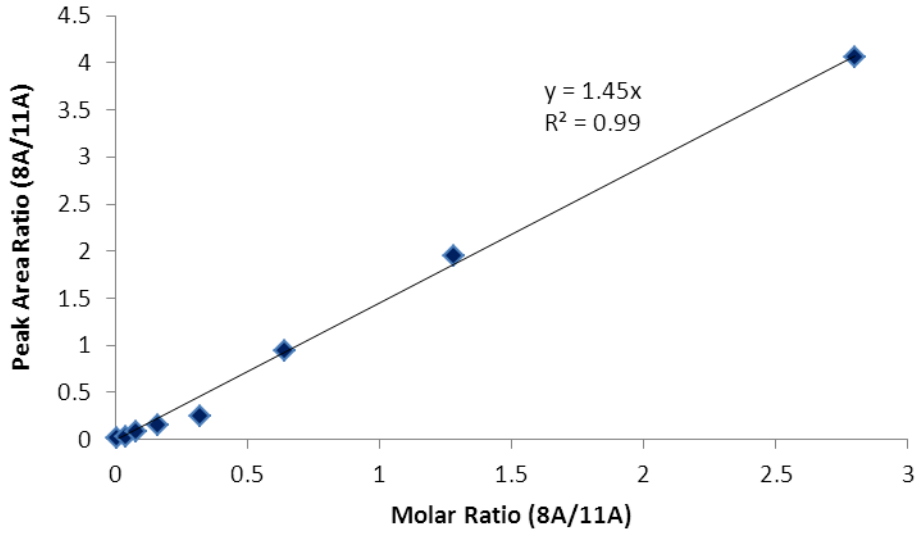
y = 1.45x
R² = 0.99
Peak Area Ratio (8A/11A)
Molar Ratio (8A/11A)
0
0.5
1
1.5
2
2.5
3
3.5
4
4.5
0
0.5
1
1.5
2
2.5
3

Figure S2.

(C)

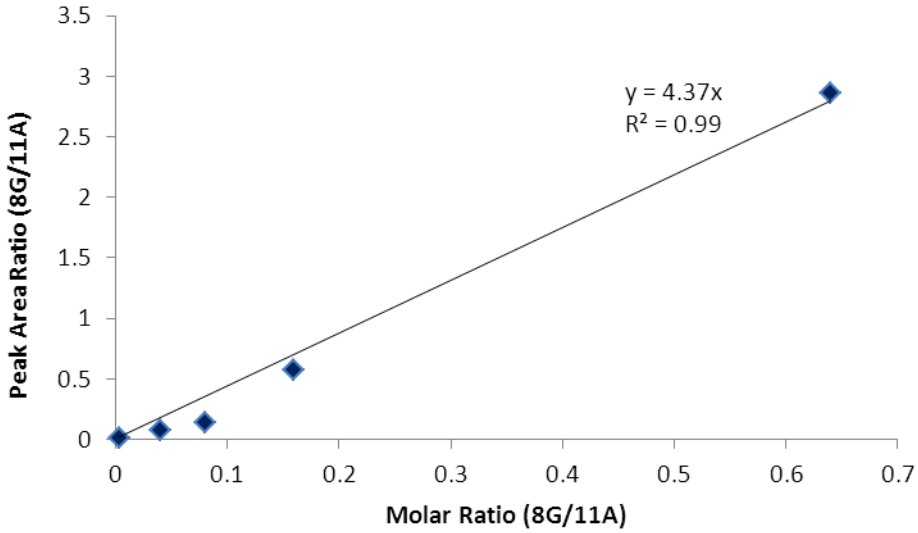
y = 4.37x
R² = 0.99
Peak Area Ratio (8G/11A)
Molar Ratio (8G/11A)
3.5
3
2.5
2
1.5
1
0.5
0
0
0.1
0.2
0.3
0.4
0.5
0.6
0.7

(D)

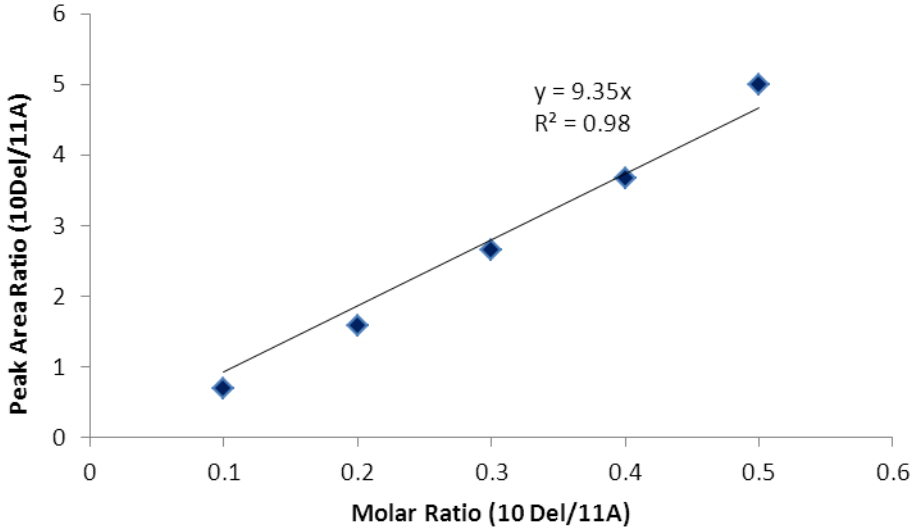
y = 9.35x
R² = 0.98
Peak Area Ratio (10Del/11A)
Molar Ratio (10 Del/11A)
6
5
4
3
2
1
0
0
0.1
0.2
0.3
0.4
0.5
0.6

Figure S2.

(E)

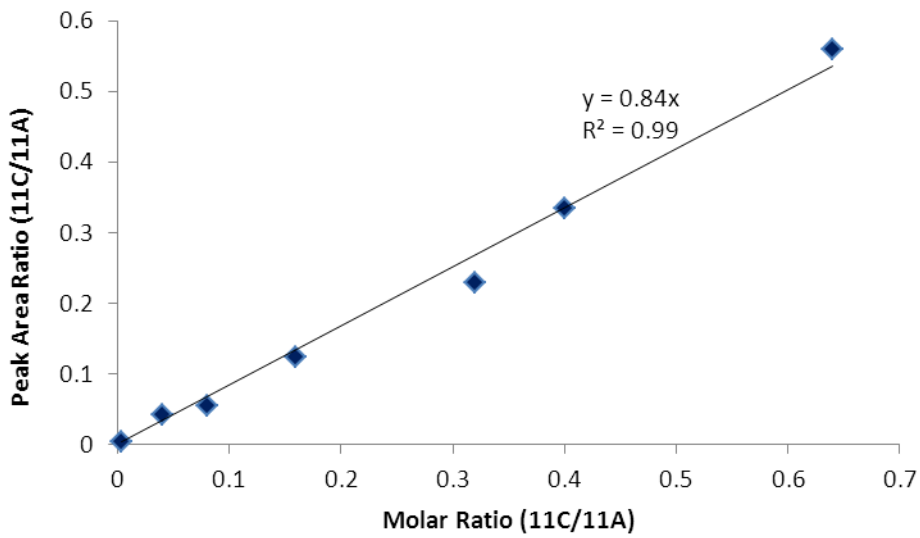
y = 0.84x
R² = 0.99
Peak Area Ratio (11C/11A)
Molar Ratio (11C/11A)
0
0.1
0.2
0.3
0.4
0.5
0.6
0.7

(F)

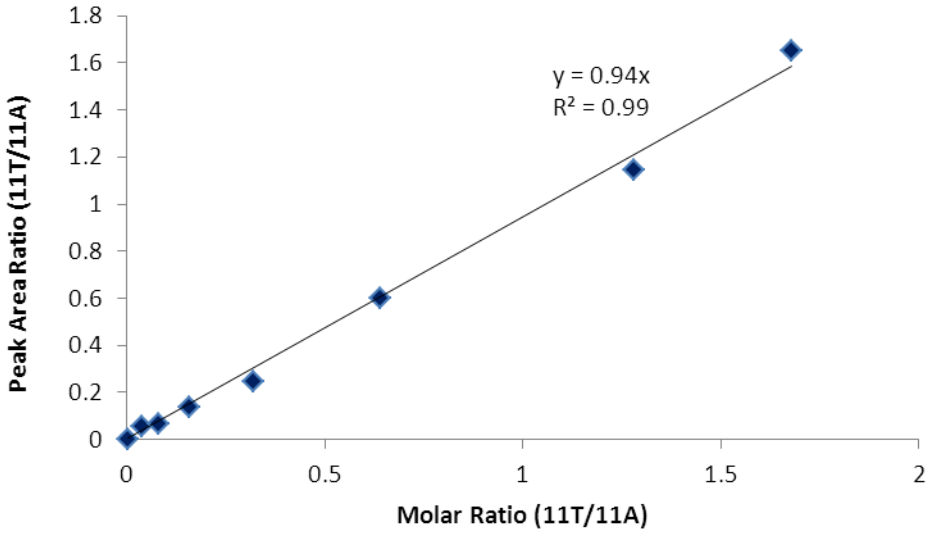
y = 0.94x
R² = 0.99
Peak Area Ratio (11T/11A)
Molar Ratio (11T/11A)
0
0.2
0.4
0.6
0.8
1
1.2
1.4
1.6
1.8
0.5
1.5
2

Figure S2.

(G)

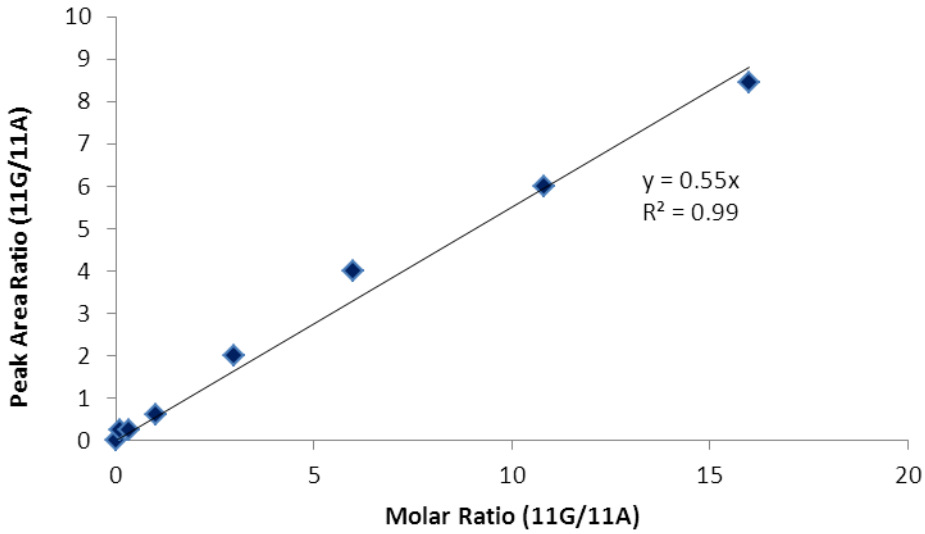
Peak Area Ratio (11G/11A)
Molar Ratio (11G/11A)
y = 0.55x
R² = 0.99
0
1
2
3
4
5
6
7
8
9
10
0
5
10
15
20

Figure S2.

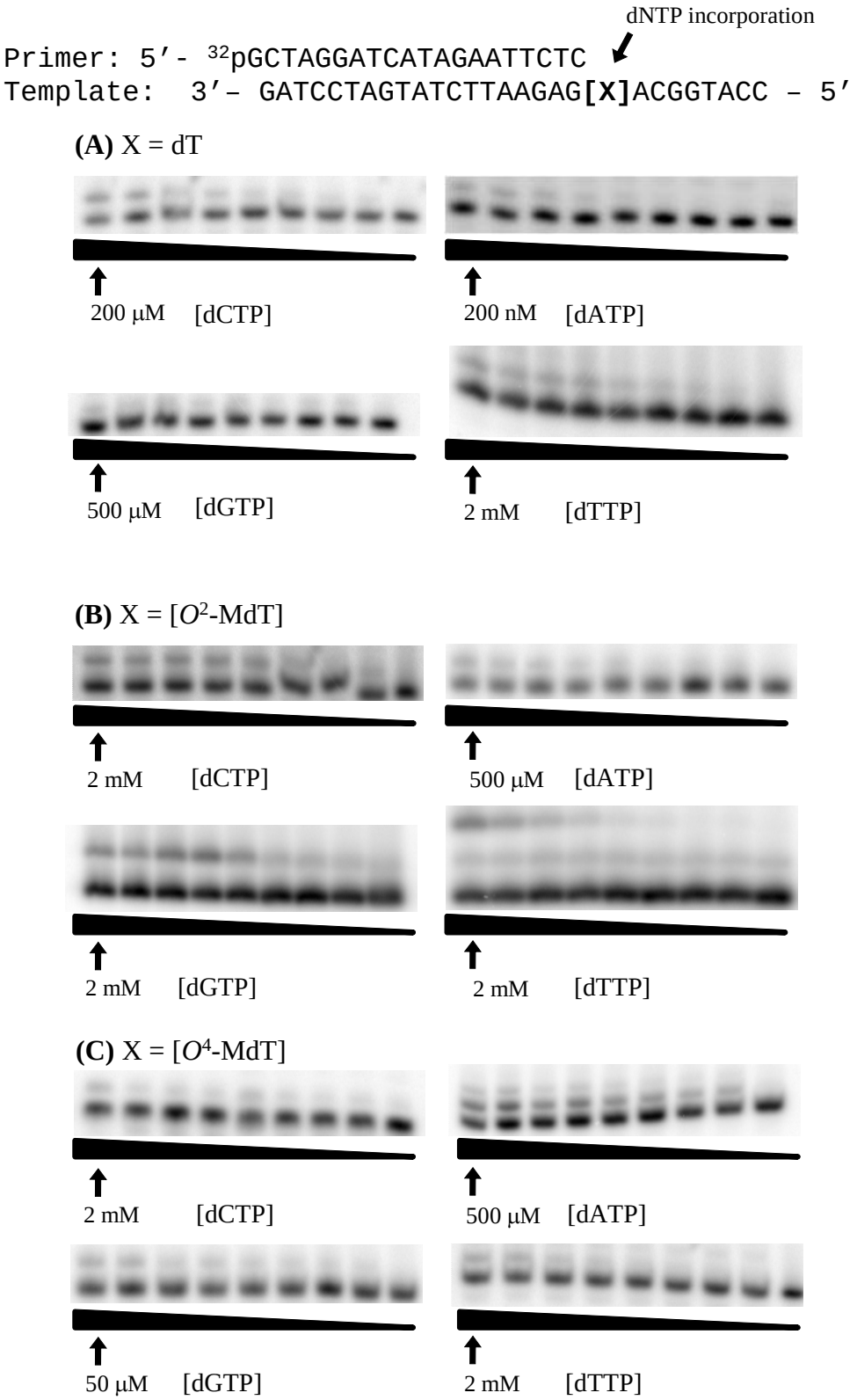
dNTP incorporation
Primer: 5′- 32pGCTAGGATCATAGAATTCTC
Template: 3′– GATCCTAGTATCTTAAGAG[X]ACGGTACC – 5′
(A) X = dT
200 μM [dCTP]
200 nM [dATP]
500 μM [dGTP]
2 mM [dTTP]
(B) X = [O2-MdT]
2 mM [dCTP]
500 μM [dATP]
2 mM [dGTP]
2 mM [dTTP]
(C) X = [O4-MdT]
2 mM [dCTP]
500 μM [dATP]
50 μM [dGTP]
2 mM [dTTP]

Figure S3.

Primer: 5′- ^{32}pGCTAGGATCATAGAATTCTC ↙
Template: 3′ – GATCCTAGTATCTTAAGAG**[X]**ACGGTACC – 5′

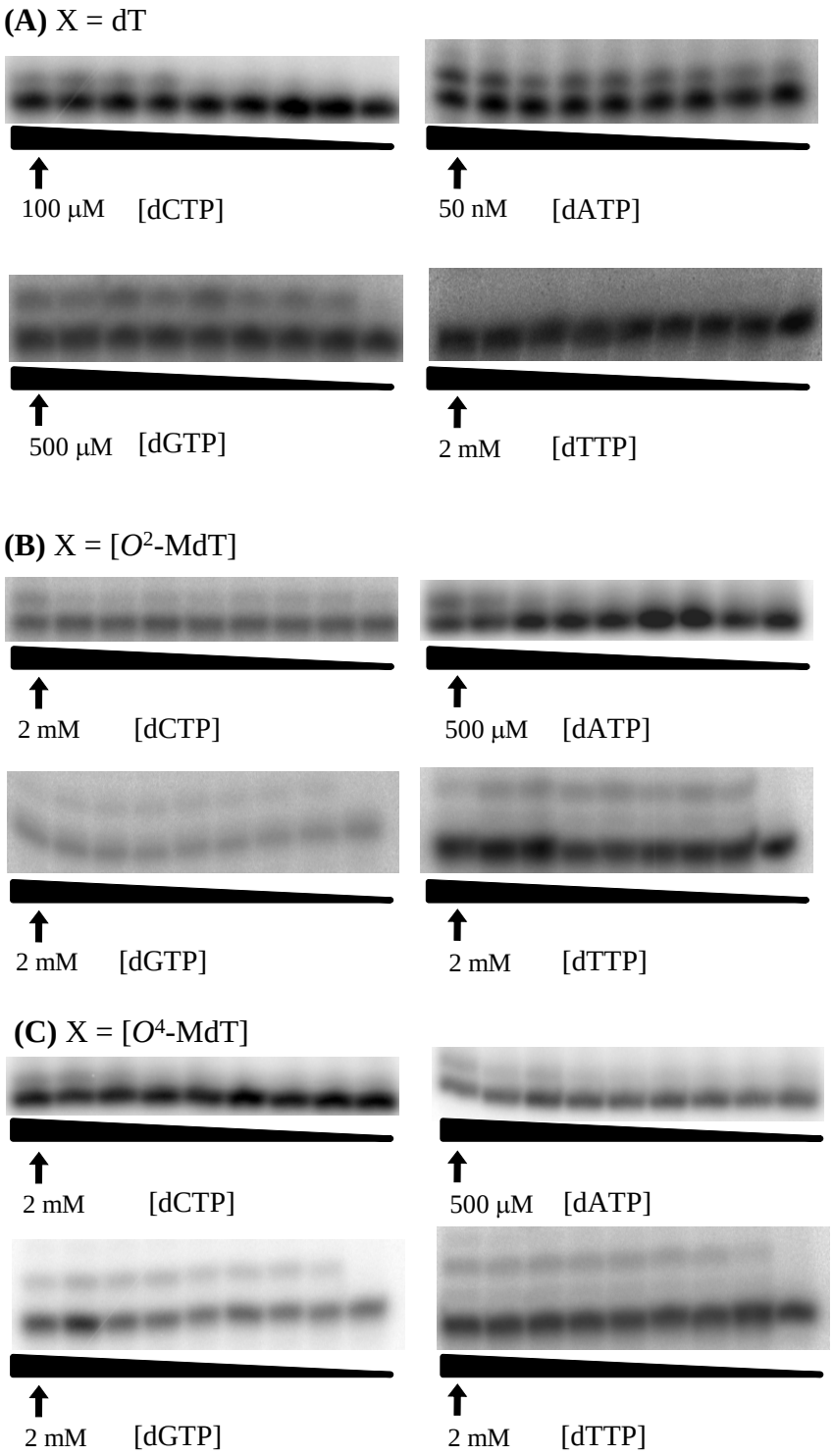

Figure S4.

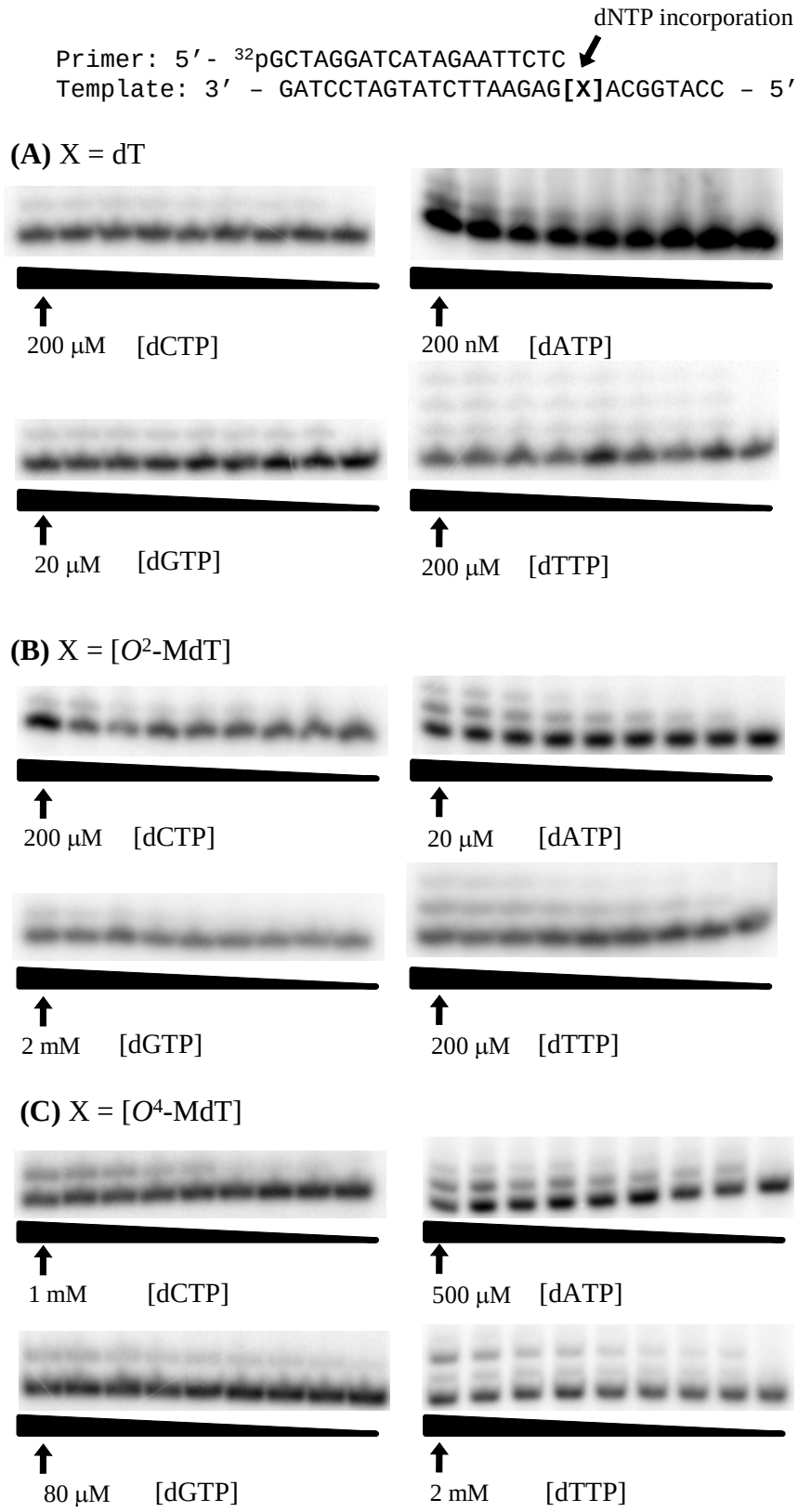
dNTP incorporation
Primer: 5′- 32pGCTAGGATCATAGAATTCTC
Template: 3′ – GATCCTAGTATCTTAAGAG[X]ACGGTACC – 5′
(A) X = dT
200 μM [dCTP]
200 nM [dATP]
20 μM [dGTP]
200 μM [dTTP]
(B) X = [O2-MdT]
200 μM [dCTP]
20 μM [dATP]
2 mM [dGTP]
200 μM [dTTP]
(C) X = [O4-MdT]
1 mM [dCTP]
500 μM [dATP]
80 μM [dGTP]
2 mM [dTTP]

Figure S5.

(A)

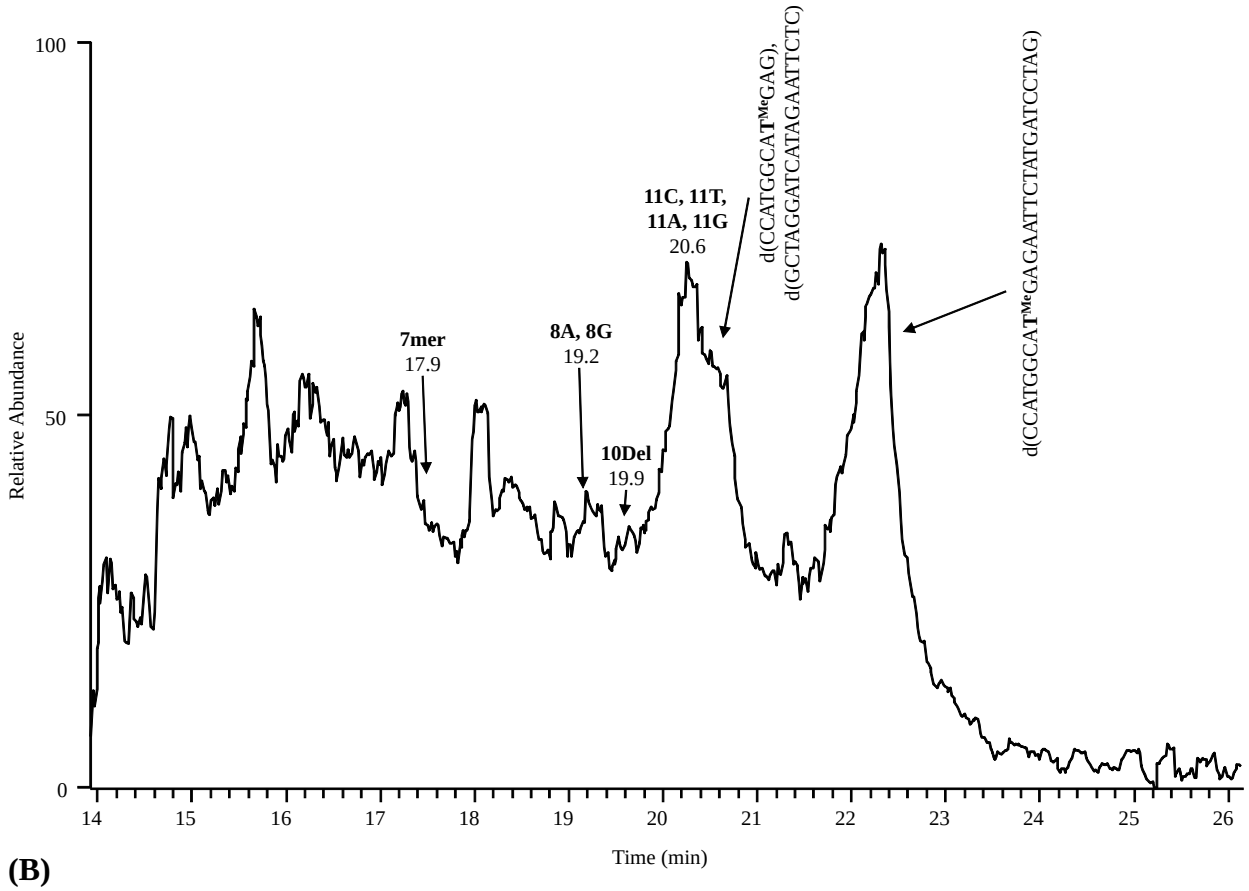
100
50
0
Relative Abundance
14
15
16
17
18
19
20
21
22
23
24
25
26
Time (min)
7mer
17.9
8A, 8G
19.2
10Del
19.9
11C, 11T,
11A, 11G
20.6
d(CCATGGCAT^MeGAG),
d(GCTAGGATCATAGAATTCTC)
d(CCATGGCAT^MeGAGAATTCTATGATCCTAG)

(B)

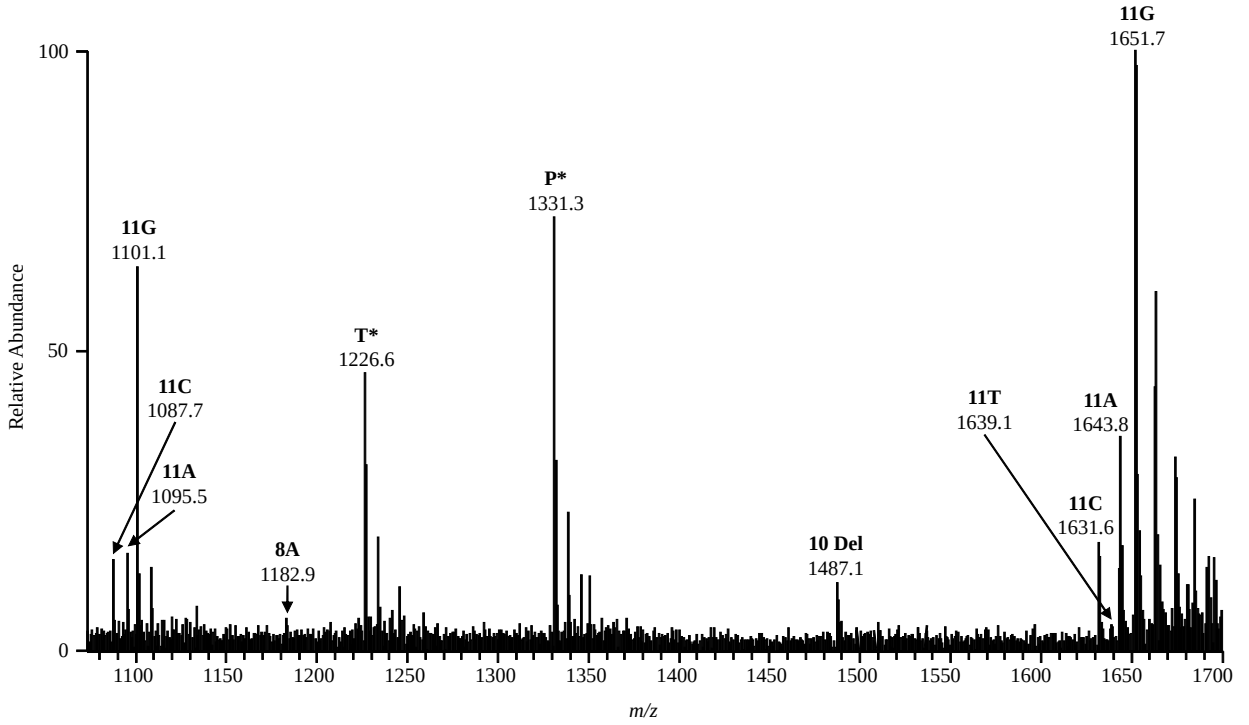
100
50
0
Relative Abundance
1100
1150
1200
1250
1300
1350
1400
1450
1500
1550
1600
1650
1700
m/z
11G
1101.1
11C
1087.7
11A
1095.5
8A
1182.9
T*
1226.6
P*
1331.3
10 Del
1487.1
11T
1639.1
11C
1631.6
11A
1643.8
11G
1651.7

Figure S6.

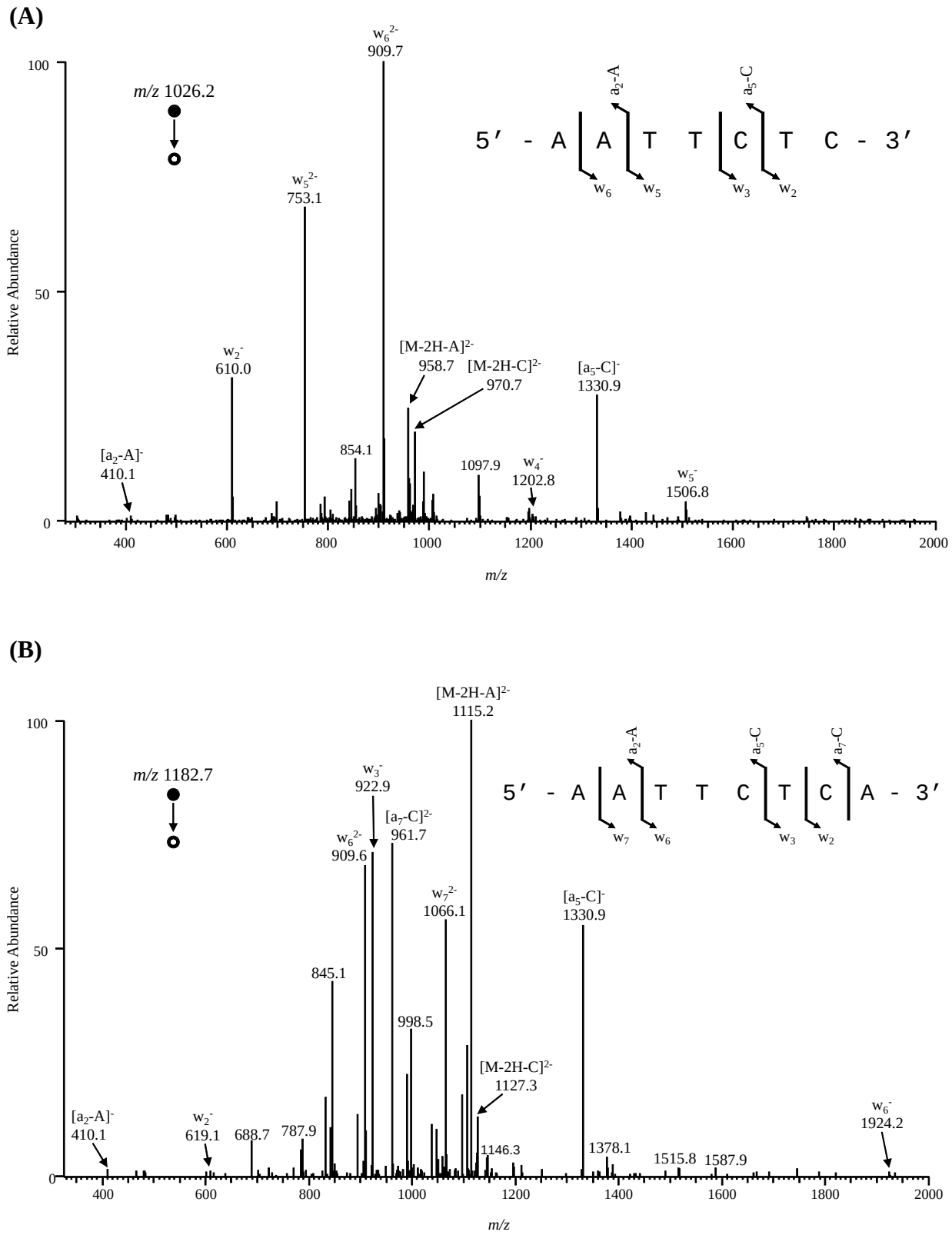
(A)
m/z 1026.2
5′ - A A T T C T C - 3′
a2-A
a5-C
w6
w5
w3
w2
w6 2- 909.7
w5 2- 753.1
w2 - 610.0
[M-2H-A]2- 958.7
[M-2H-C]2- 970.7
[a5-C]- 1330.9
[a2-A]- 410.1
854.1
1097.9
w4 - 1202.8
w5 - 1506.8
Relative Abundance
m/z
(B)
m/z 1182.7
5′ - A A T T C T C A - 3′
a2-A
a5-C
a7-C
w7
w6
w3
w2
[M-2H-A]2- 1115.2
w3 - 922.9
[a7-C]2- 961.7
w6 2- 909.6
w7 2- 1066.1
[a5-C]- 1330.9
845.1
998.5
[M-2H-C]2- 1127.3
[a2-A]- 410.1
w2 - 619.1
688.7
787.9
1146.3
1378.1
1515.8
1587.9
w6 - 1924.2
Relative Abundance
m/z

Figure S7.

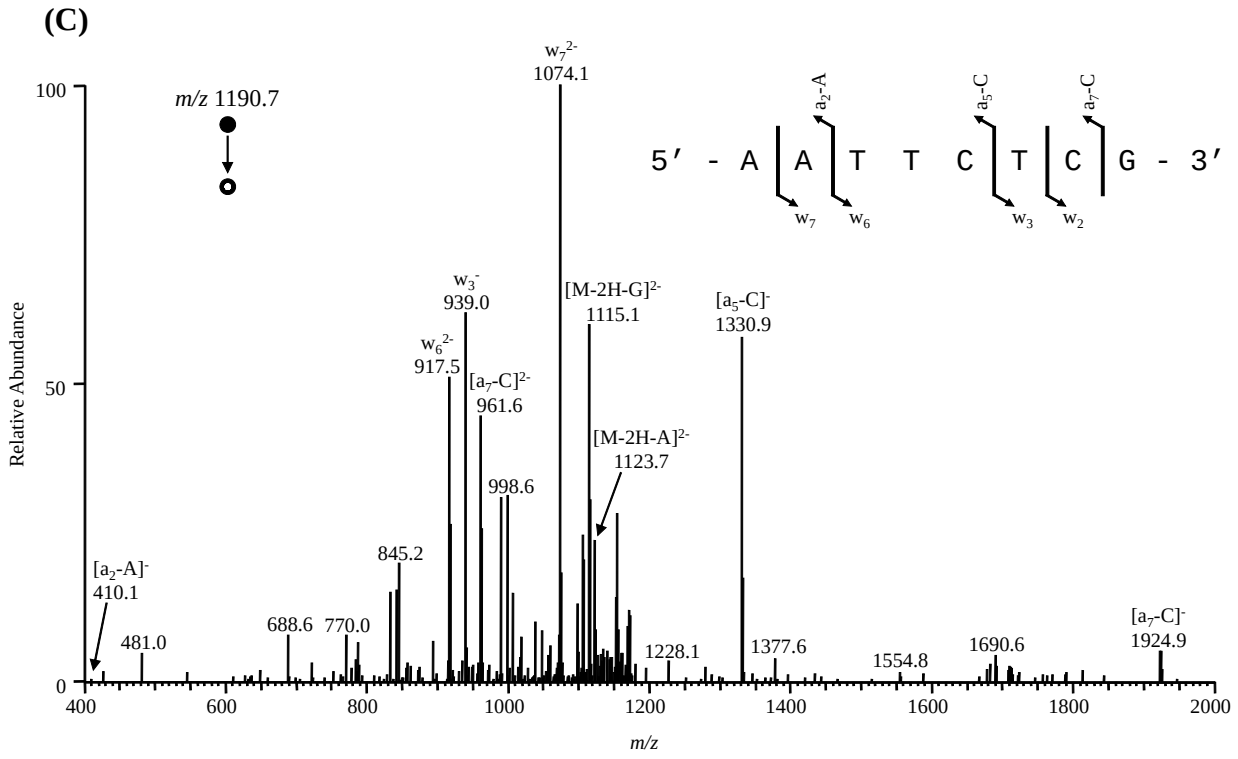
(C)
m/z 1190.7
5′ - A A T T C T C G - 3′
w7
w6
w3
w2
a2-A
a5-C
a7-C
w7 2- 1074.1
w3- 939.0
w6 2- 917.5
[a7-C]2- 961.6
[M-2H-G]2- 1115.1
[M-2H-A]2- 1123.7
998.6
845.2
[a5-C]- 1330.9
[a2-A]- 410.1
481.0
688.6
770.0
1228.1
1377.6
1554.8
1690.6
[a7-C]- 1924.9
Relative Abundance
m/z

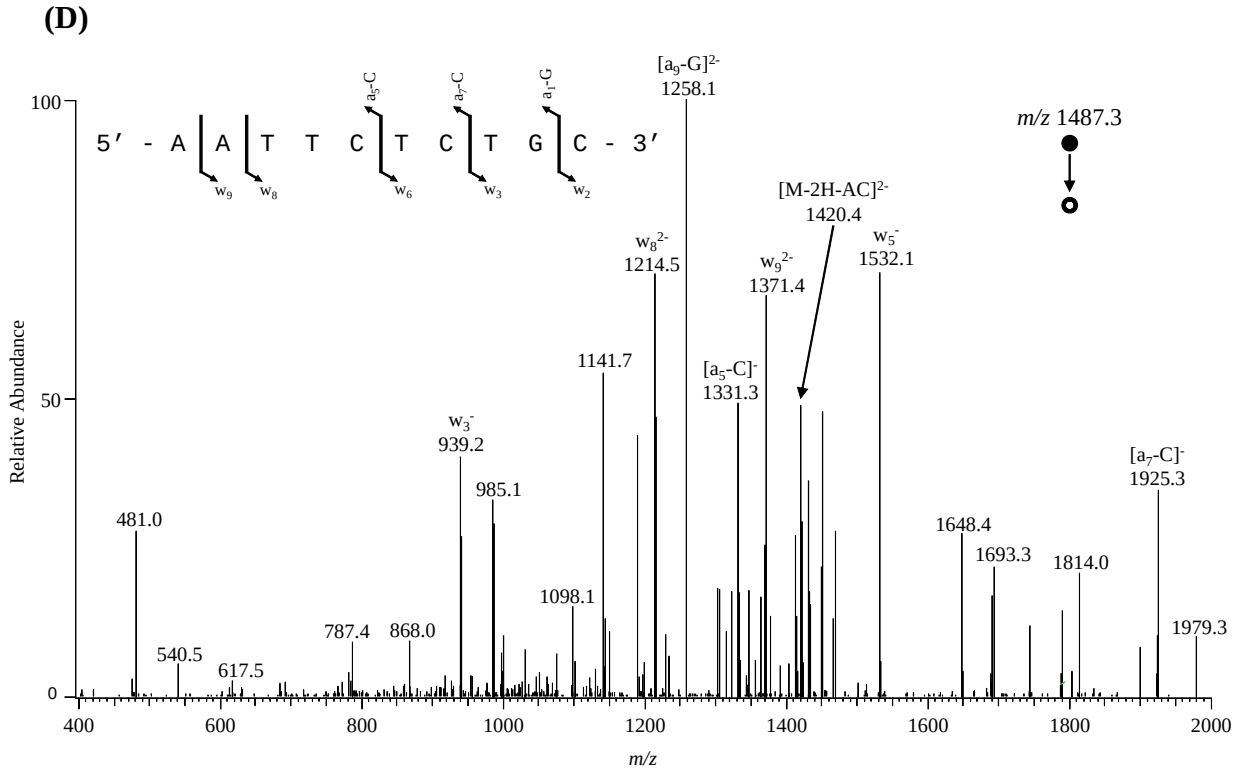
(D)
5′ - A A T T C T C T G C - 3′
w9
w8
w6
w3
w2
a5-C
a7-C
a1-G
m/z 1487.3
[a9-G]2- 1258.1
[M-2H-AC]2- 1420.4
w8 2- 1214.5
w9 2- 1371.4
w5- 1532.1
1141.7
[a5-C]- 1331.3
w3- 939.2
985.1
481.0
1098.1
787.4
868.0
540.5
617.5
1648.4
1693.3
1814.0
[a7-C]- 1925.3
1979.3
Relative Abundance
m/z

Figure S7.

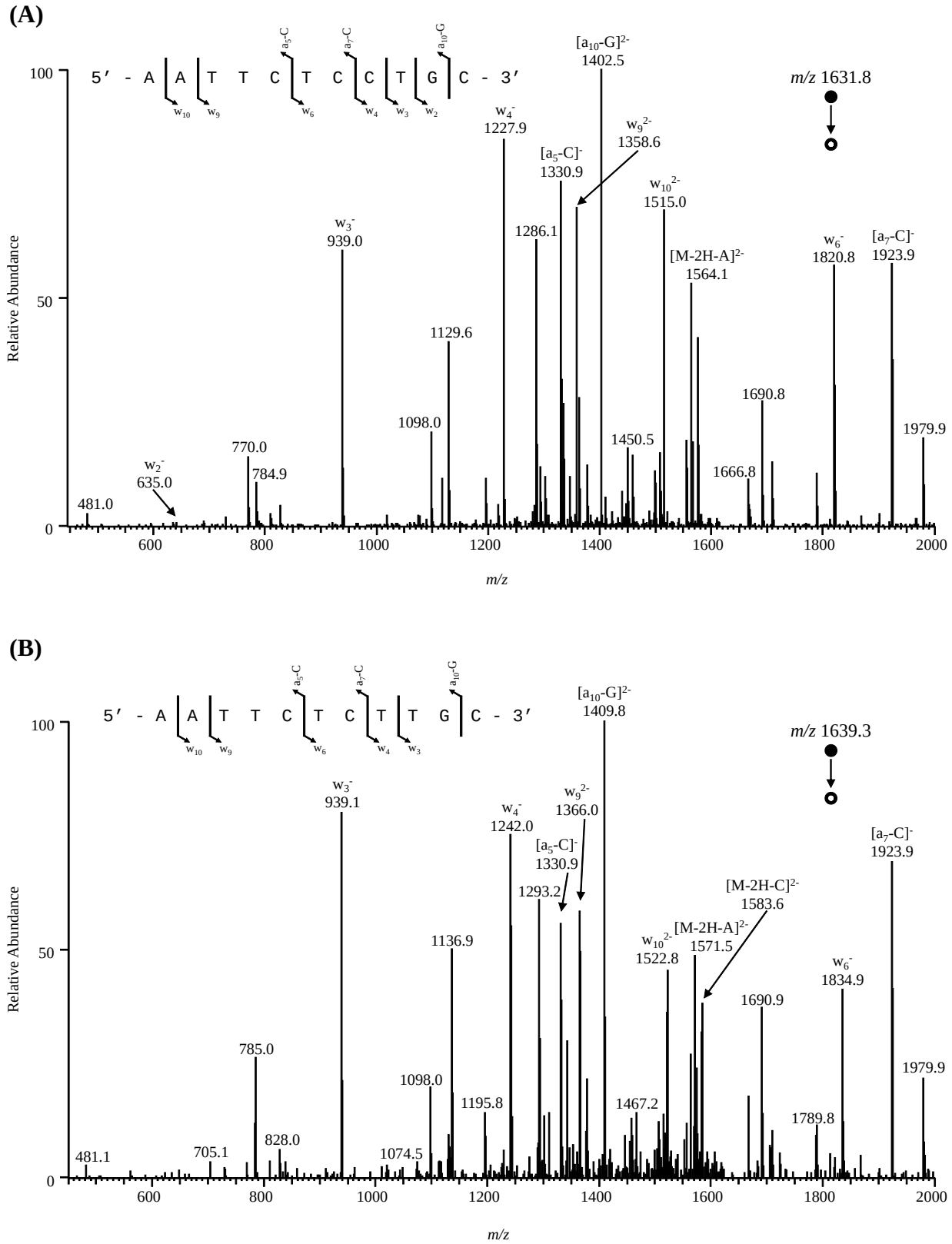
(A)
5′ - A A T T C T C C T G C - 3′
m/z 1631.8
[a10-G]2- 1402.5
w4- 1227.9
w92- 1358.6
[a5-C]- 1330.9
w102- 1515.0
w3- 939.0
1286.1
[M-2H-A]2- 1564.1
w6- 1820.8
[a7-C]- 1923.9
1129.6
1690.8
1098.0
1979.9
1450.5
770.0
w2- 635.0
784.9
1666.8
481.0
Relative Abundance
m/z
(B)
5′ - A A T T C T C T T G C - 3′
m/z 1639.3
[a10-G]2- 1409.8
w3- 939.1
w92- 1366.0
w4- 1242.0
[a5-C]- 1330.9
[a7-C]- 1923.9
1293.2
[M-2H-C]2- 1583.6
[M-2H-A]2- 1571.5
w102- 1522.8
1136.9
w6- 1834.9
1690.9
785.0
1979.9
1098.0
1195.8
1467.2
1789.8
828.0
481.1
705.1
1074.5
Relative Abundance
m/z

Figure S8.

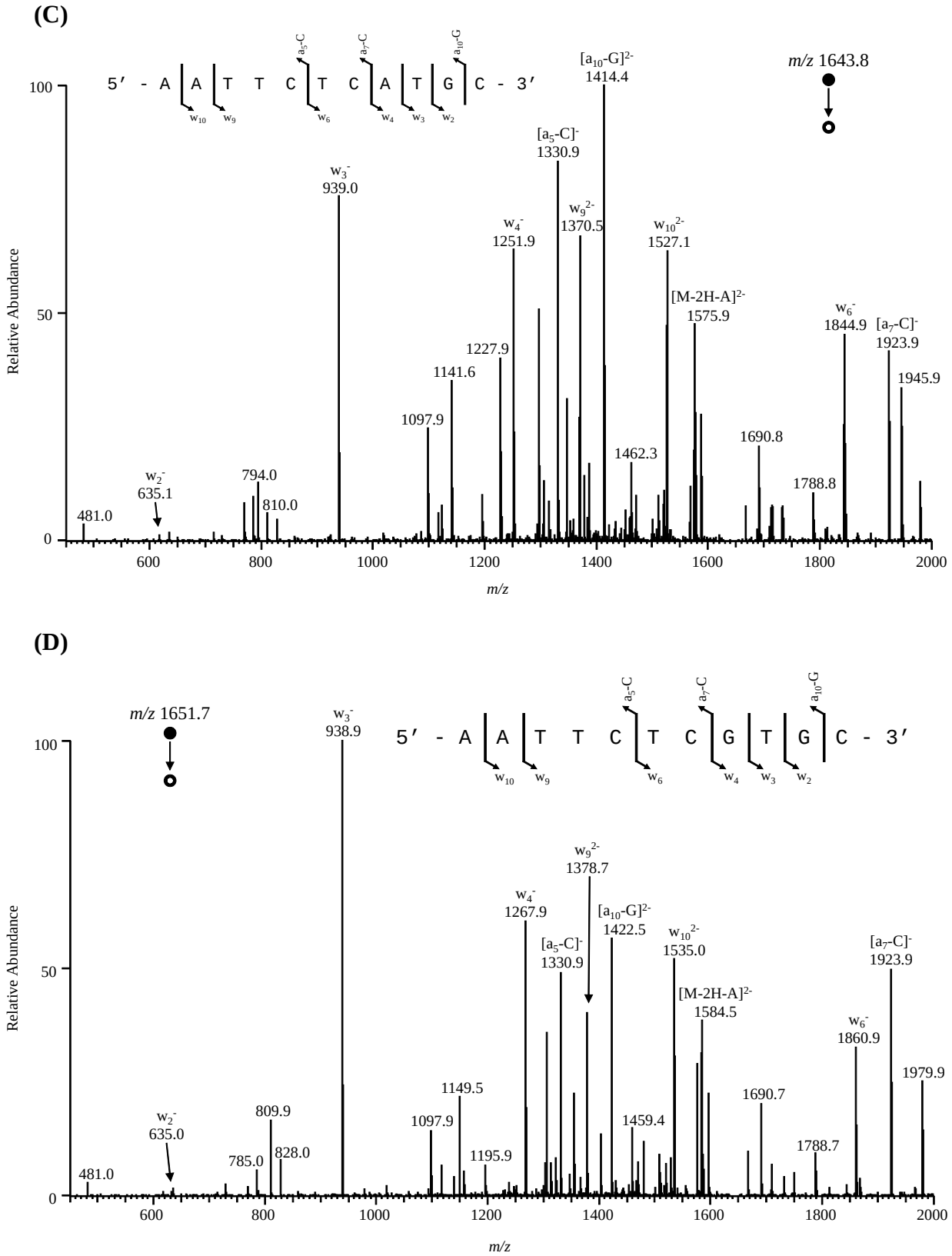
(C)
5′ - A A T T C T C A T G C - 3′
m/z 1643.8
[a10-G]2- 1414.4
[a5-C]- 1330.9
w3- 939.0
w9 2- 1370.5
w4- 1251.9
w10 2- 1527.1
[M-2H-A]2- 1575.9
w6- 1844.9
[a7-C]- 1923.9
1945.9
1227.9
1141.6
1097.9
1690.8
1462.3
1788.8
w2- 635.1
794.0
810.0
481.0
Relative Abundance
m/z
(D)
m/z 1651.7
w3- 938.9
5′ - A A T T C T C G T G C - 3′
w9 2- 1378.7
w4- 1267.9
[a10-G]2- 1422.5
w10 2- 1535.0
[a5-C]- 1330.9
[a7-C]- 1923.9
[M-2H-A]2- 1584.5
w6- 1860.9
1979.9
1149.5
1690.7
1097.9
1459.4
w2- 635.0
809.9
1788.7
785.0
828.0
1195.9
481.0
Relative Abundance
m/z

Figure S8.

(A)

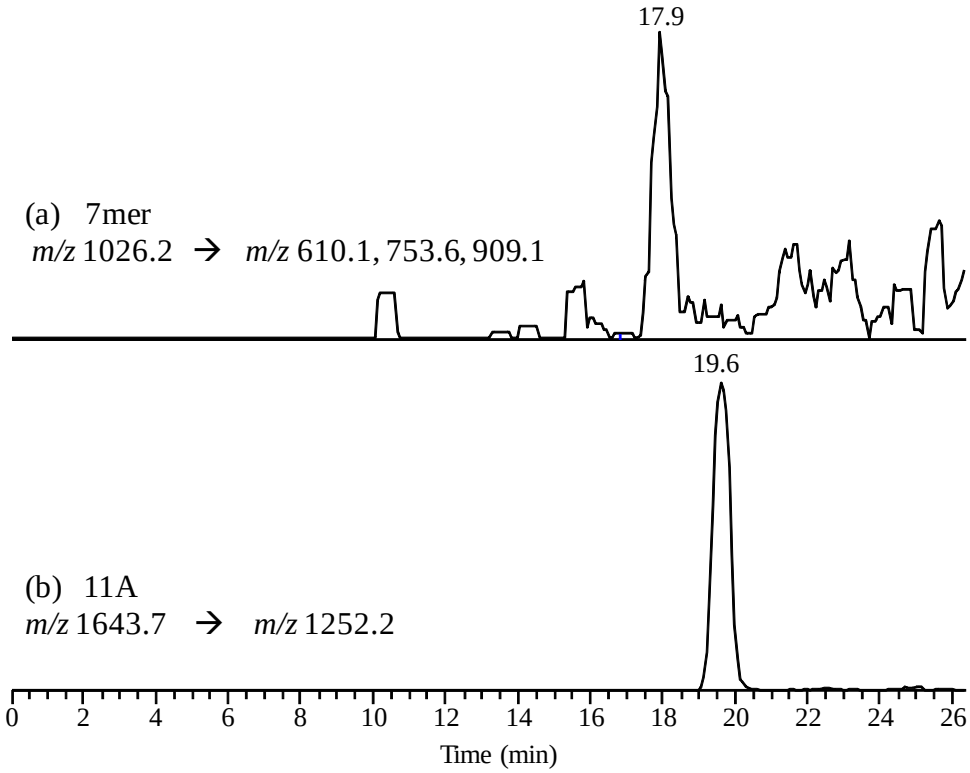


```
5′- GC AXG AGA ATT -3′
    3′-  C TCT TAA -5′     7mer     2%
3′- CG TAC TCT TAA -5′     11A      98%
```

dT Replication From Klenow fragment exo⁻

Figure S9.

(B)

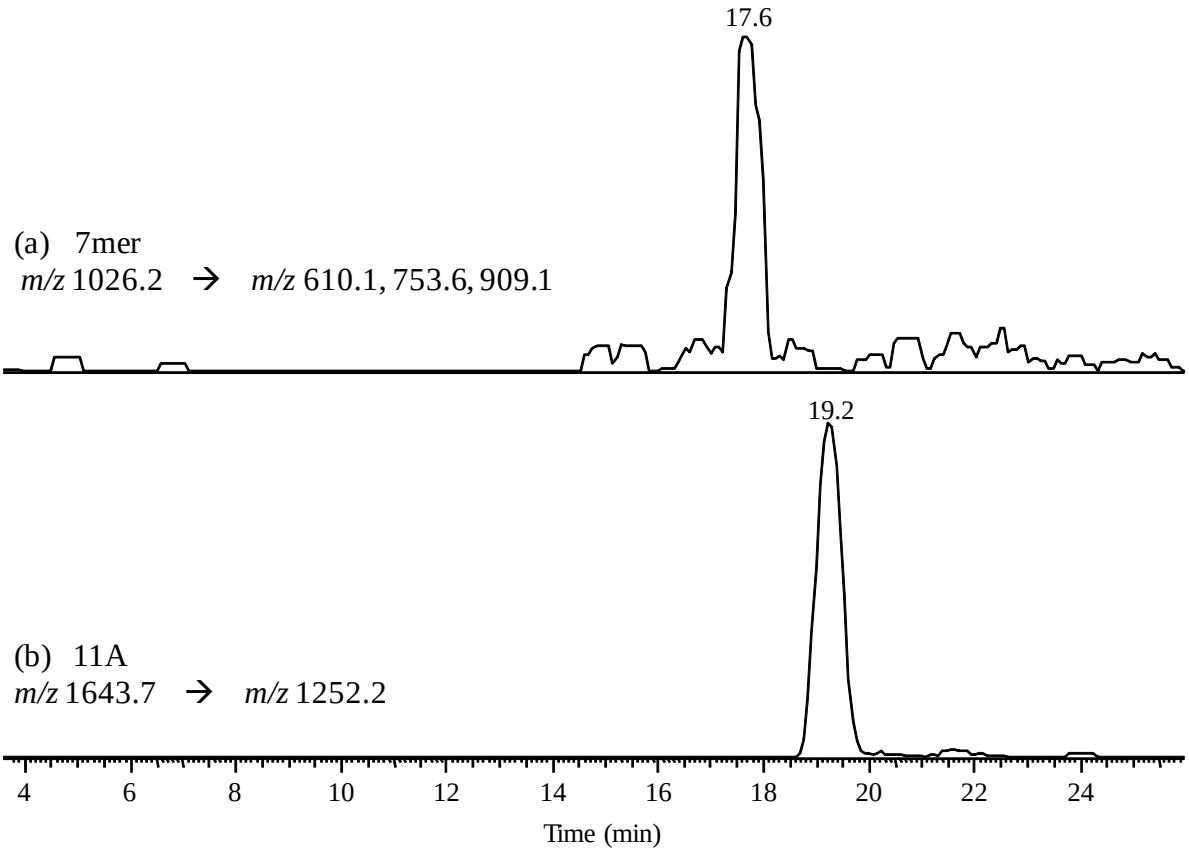


```
5′- GC AXG AGA ATT -3′
    3′-  C TCT TAA -5′     7mer     4%
3′- CG TAC TCT TAA -5′     11A      96%
```

dT Replication From pol η

Figure S9.

(C)

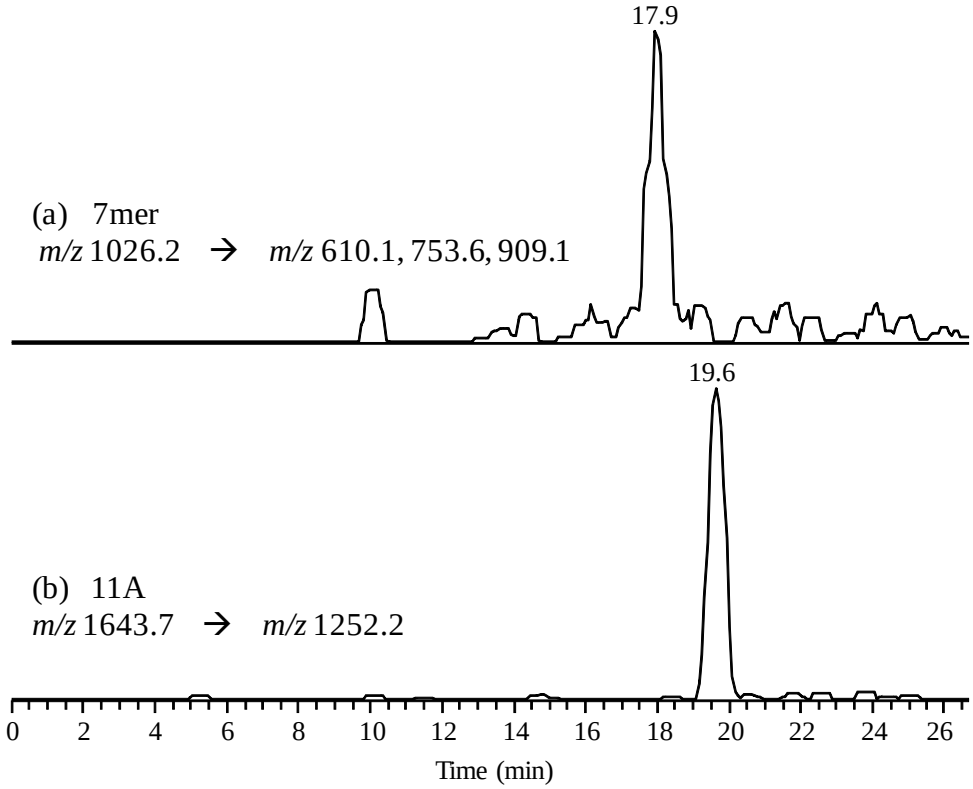


```
5′- GC AXG AGA ATT -3′
    3′-  C TCT TAA -5′     7mer     1%
3′- CG TAC TCT TAA -5′     11A      99%
```

dT Replication From pol κ

Figure S9.

(A)

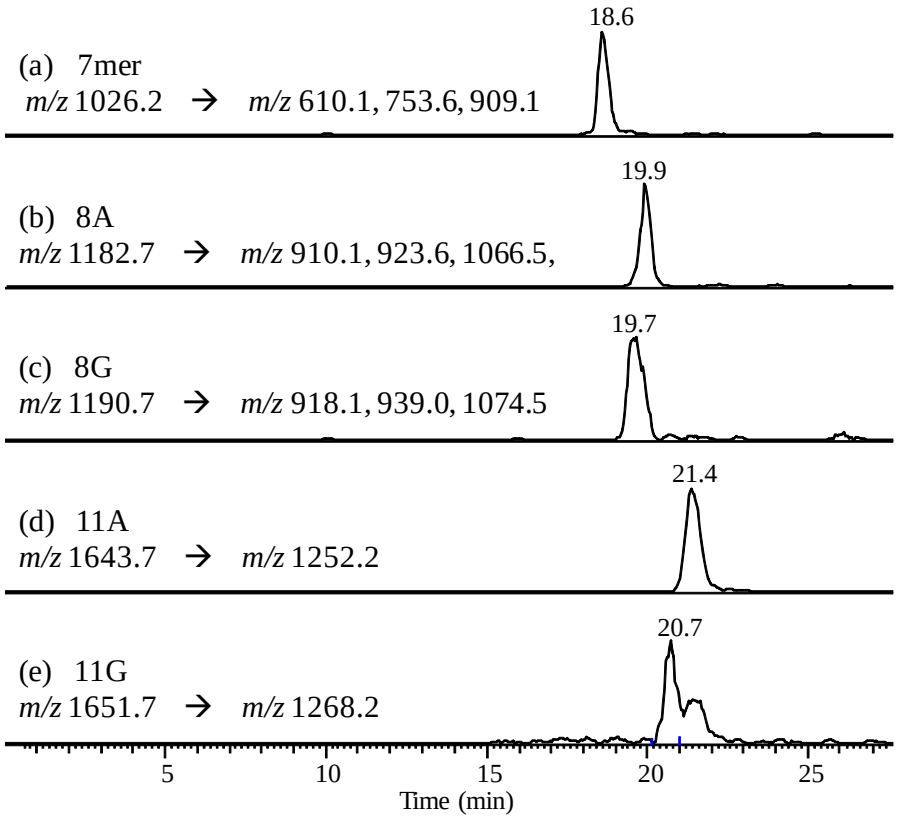


```
5′- GC AXG AGA ATT -3′
    3′-  C TCT TAA -5′     7mer     2%
   3′-  AC TCT TAA -5′     8A       9%
   3′-  GC TCT TAA -5′     8G       4%
3′- CG TAC TCT TAA -5′     11A      77%
3′- CG TGC TCT TAA -5′     11G      7%
```

O^2-MdT Replication From Klenow fragment exo$^-$

Figure S10.

(B)

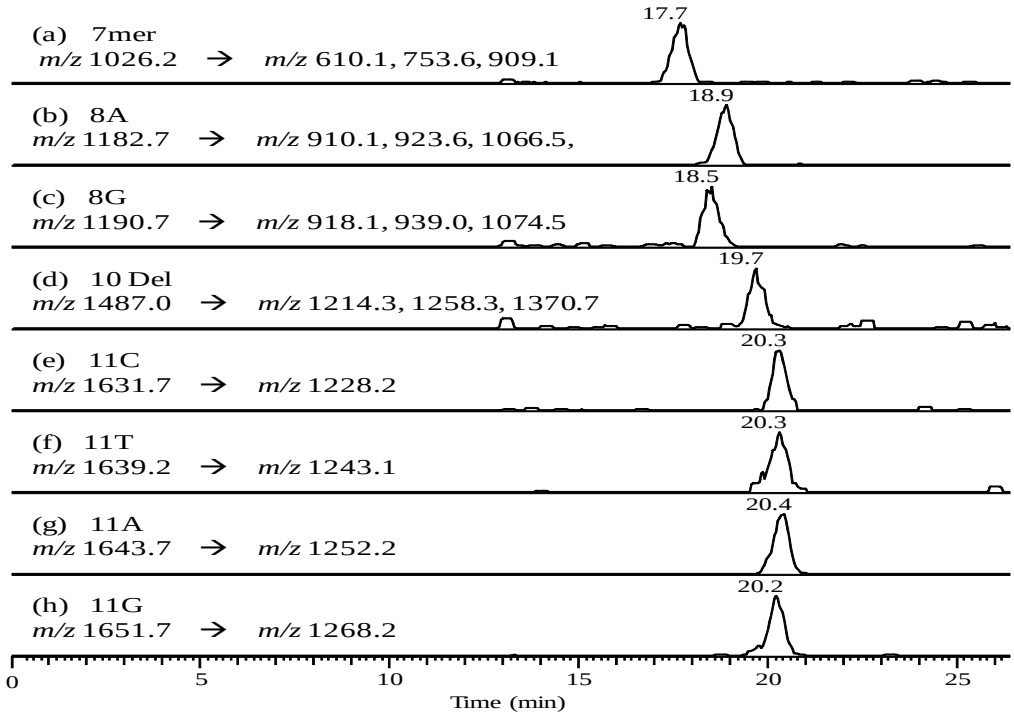

5′- GC AXG AGA ATT -3′		
3′- C TCT TAA -5′	**7mer**	**6%**
3′- AC TCT TAA -5′	**8A**	**2%**
3′- GC TCT TAA -5′	**8G**	**6%**
3′- CG T C TCT TAA -5′	**10Del**	**1%**
3′- CG TCC TCT TAA -5′	**11C**	**5%**
3′- CG TTC TCT TAA -5′	**11T**	**6%**
3′- CG TAC TCT TAA -5′	**11A**	**45%**
3′- CG TGC TCT TAA -5′	**11G**	**27%**

***O*²-MdT Replication From pol η**

Figure S10.

(A)

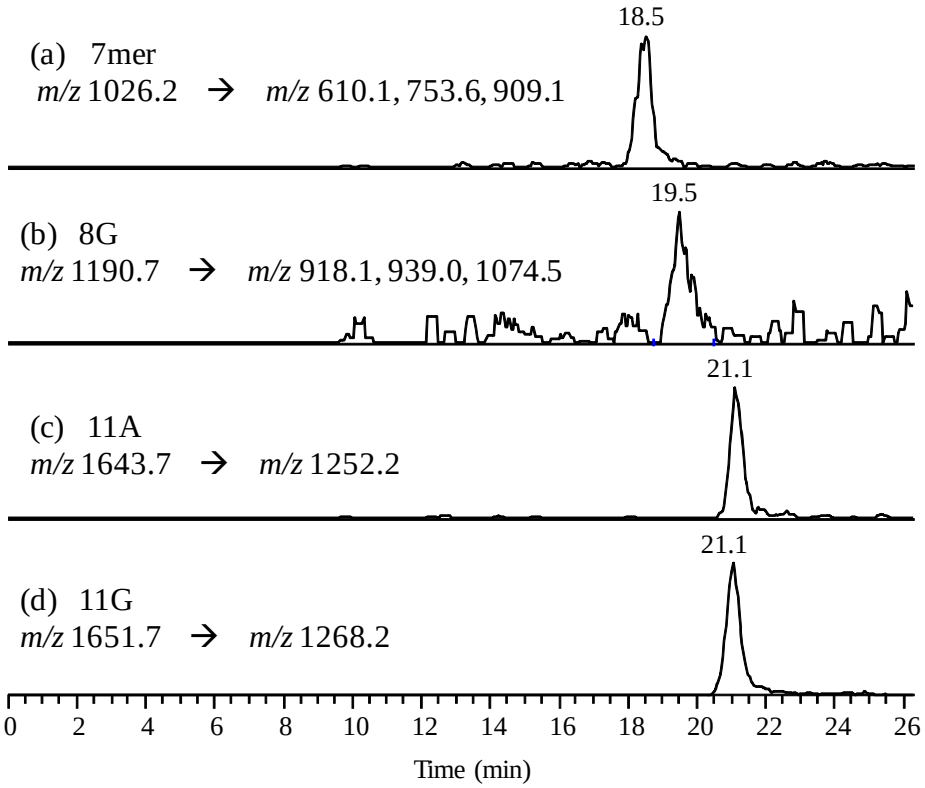

5′- GC A**X**G AGA ATT -3′		
3′- C TCT TAA -5′	**7mer**	**7%**
3′- GC TCT TAA -5′	**8G**	**5%**
3′- CG TAC TCT TAA -5′	**11A**	**7%**
3′- CG TGC TCT TAA -5′	**11G**	**80%**

O^4-MdT Replication From Klenow fragment exo$^-$

Figure S11.

(B)

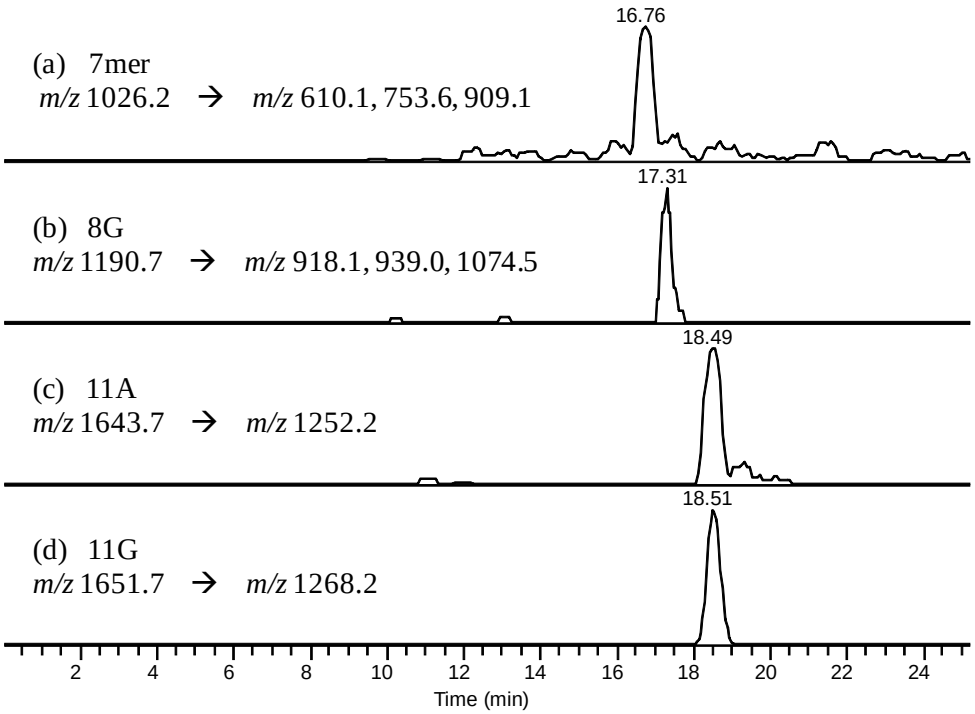

5′- GC A**X**G AGA ATT -3′		
3′- C TCT TAA -5′	**7mer**	**6%**
3′- GC TCT TAA -5′	**8G**	**2%**
3′- CG TAC TCT TAA -5′	**11A**	**9%**
3′- CG TGC TCT TAA -5′	**11G**	**83%**

***O*⁴-MdT Replication From pol η**

Figure S11.

(C)

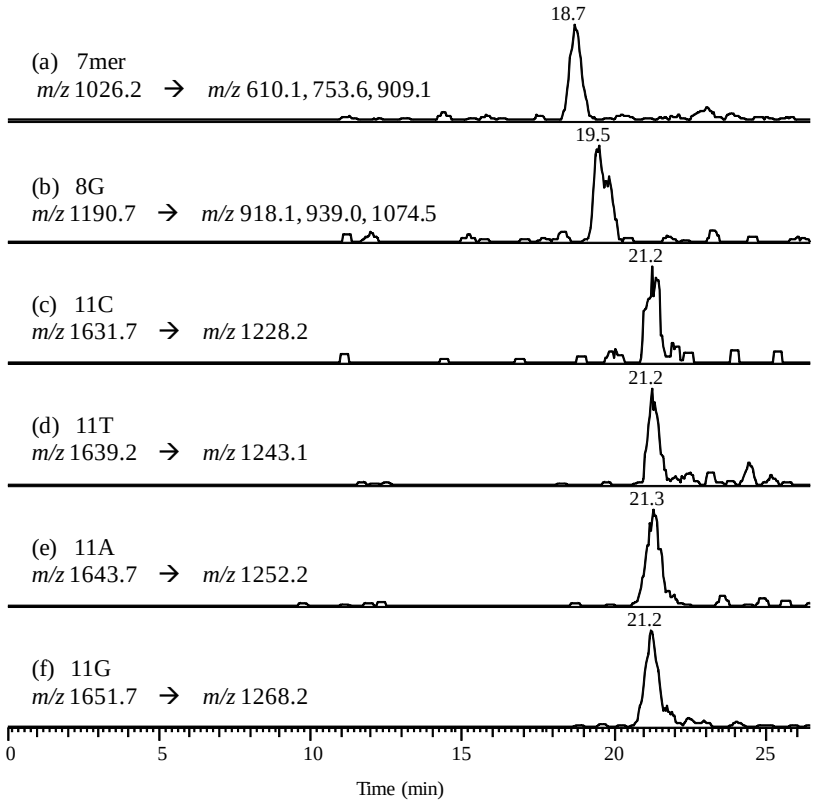


```
5′- GC AXG AGA ATT -3′
    3′-  C TCT TAA -5′    7mer    11%
   3′-  GC TCT TAA -5′    8G      18%
3′- CG TCC TCT TAA -5′    11C     2%
3′- CG TTC TCT TAA -5′    11T     3%
3′- CG TAC TCT TAA -5′    11A     8%
3′- CG TGC TCT TAA -5′    11G     58%
```

***O*⁴-MdT Replication From polκ**

Figure S11.

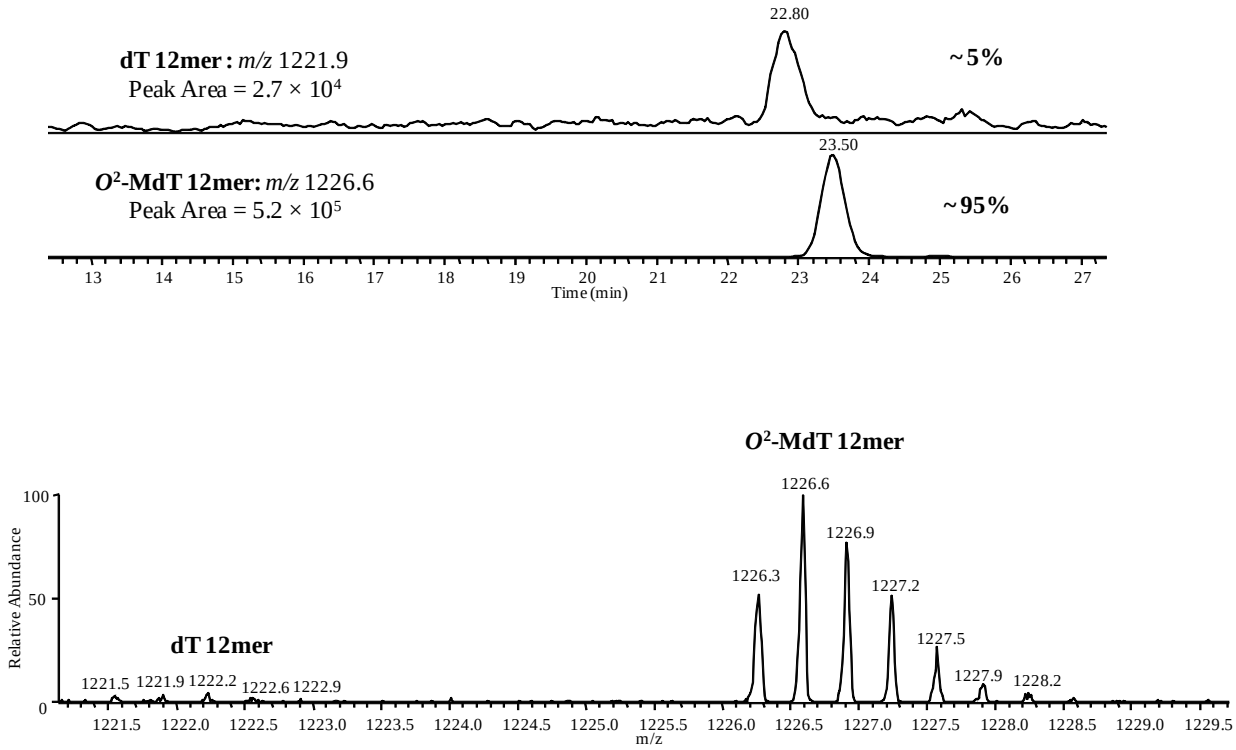
22.80
dT 12mer : m/z 1221.9
Peak Area = 2.7 × 10⁴
~5%
23.50
O²-MdT 12mer: m/z 1226.6
Peak Area = 5.2 × 10⁵
~95%
13 14 15 16 17 18 19 20 21 22 23 24 25 26 27
Time (min)
O²-MdT 12mer
1226.6
1226.9
1226.3
1227.2
1227.5
1227.9
1228.2
dT 12mer
1221.5 1221.9 1222.2 1222.6 1222.9
Relative Abundance
100
50
0
1221.5 1222.0 1222.5 1223.0 1223.5 1224.0 1224.5 1225.0 1225.5 1226.0 1226.5 1227.0 1227.5 1228.0 1228.5 1229.0 1229.5
m/z

Figure S12.

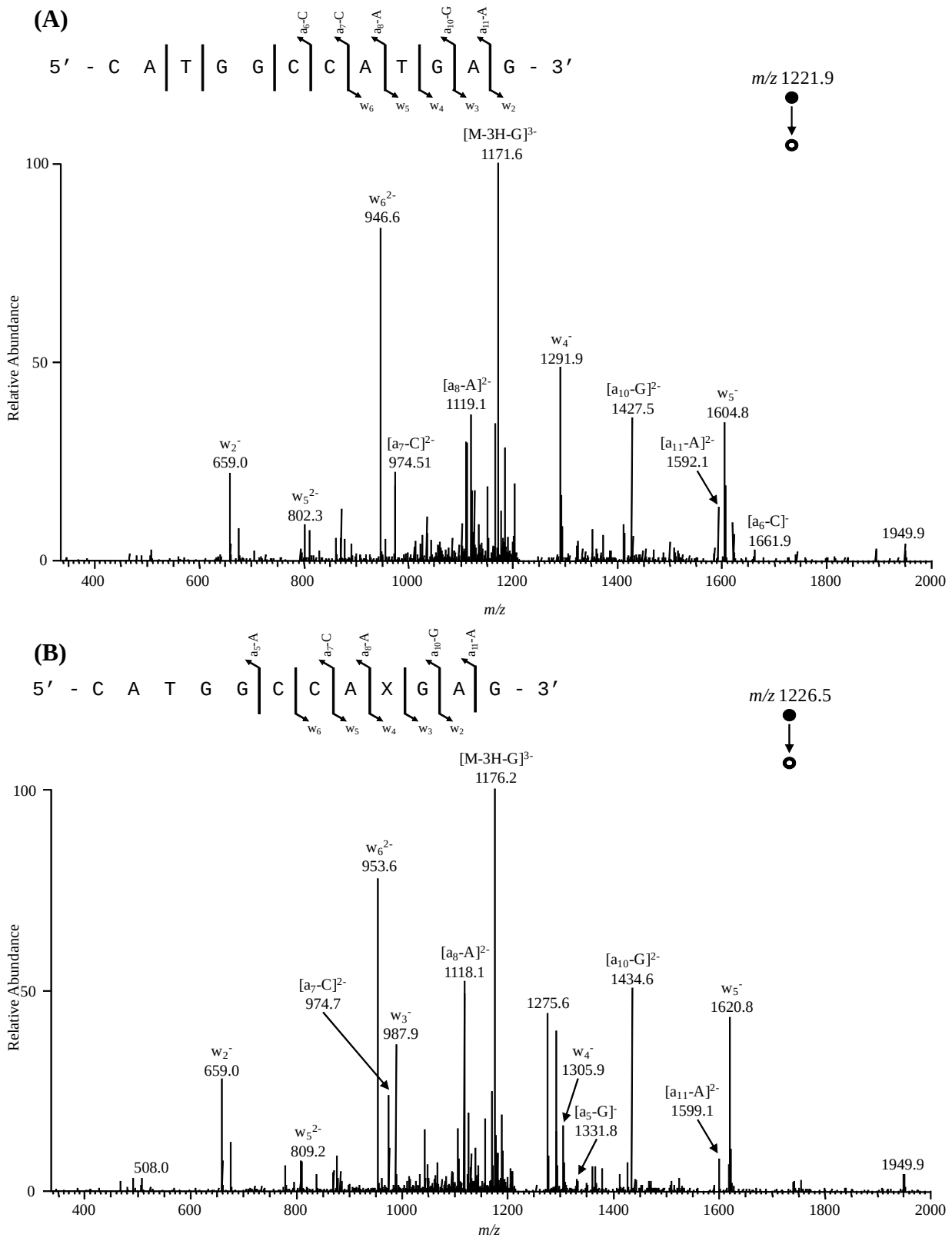
(A)
5′ - C A T G G C C A T G A G - 3′
a6-C
a7-C
a8-A
a10-G
a11-A
w6
w5
w4
w3
w2
m/z 1221.9
[M-3H-G]3-
1171.6
w62-
946.6
w4-
1291.9
[a8-A]2-
1119.1
[a10-G]2-
1427.5
w5-
1604.8
w2-
659.0
[a7-C]2-
974.51
[a11-A]2-
1592.1
w52-
802.3
[a6-C]-
1661.9
1949.9
Relative Abundance
m/z
(B)
5′ - C A T G G C C A X G A G - 3′
a5-A
a7-C
a8-A
a10-G
a11-A
m/z 1226.5
[M-3H-G]3-
1176.2
w62-
953.6
[a8-A]2-
1118.1
[a10-G]2-
1434.6
[a7-C]2-
974.7
1275.6
w5-
1620.8
w3-
987.9
w2-
659.0
w4-
1305.9
[a11-A]2-
1599.1
[a5-G]-
1331.8
w52-
809.2
508.0
1949.9
Relative Abundance
m/z

Figure S13

(A)

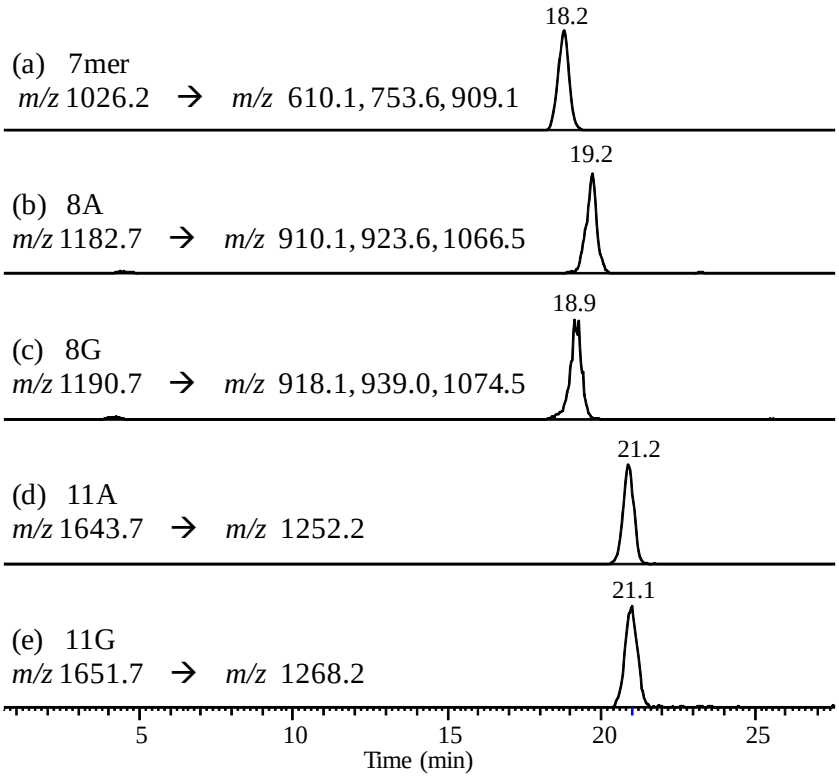


```
5′- GC AXG AGA ATT -3′
    3′-  C TCT TAA -5′    7mer    5%
   3′-  AC TCT TAA -5′    8A      3%
   3′-  GC TCT TAA -5′    8G      8%
3′- CG TAC TCT TAA -5′    11A     10%
3′- CG TGC TCT TAA -5′    11G     73%
```

O^4-MdT Replication From pol η (low dNTPs)

Figure S14.

(B)

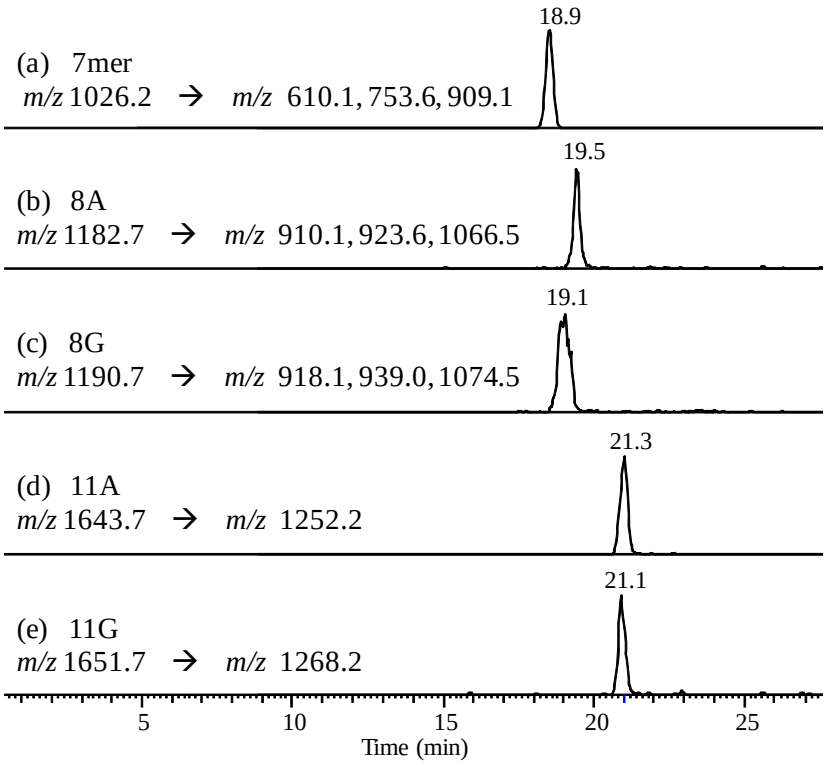


```
5′- GC AXG AGA ATT -3′
    3′-  C TCT TAA -5′    7mer    26%
   3′-  AC TCT TAA -5′    8A      3%
   3′-  GC TCT TAA -5′    8G      7%
3′- CG TAC TCT TAA -5′    11A     3%
3′- CG TGC TCT TAA -5′    11G     62%
```

***O*⁴-MdT Replication From pol η (6 hr)**

Figure S14.

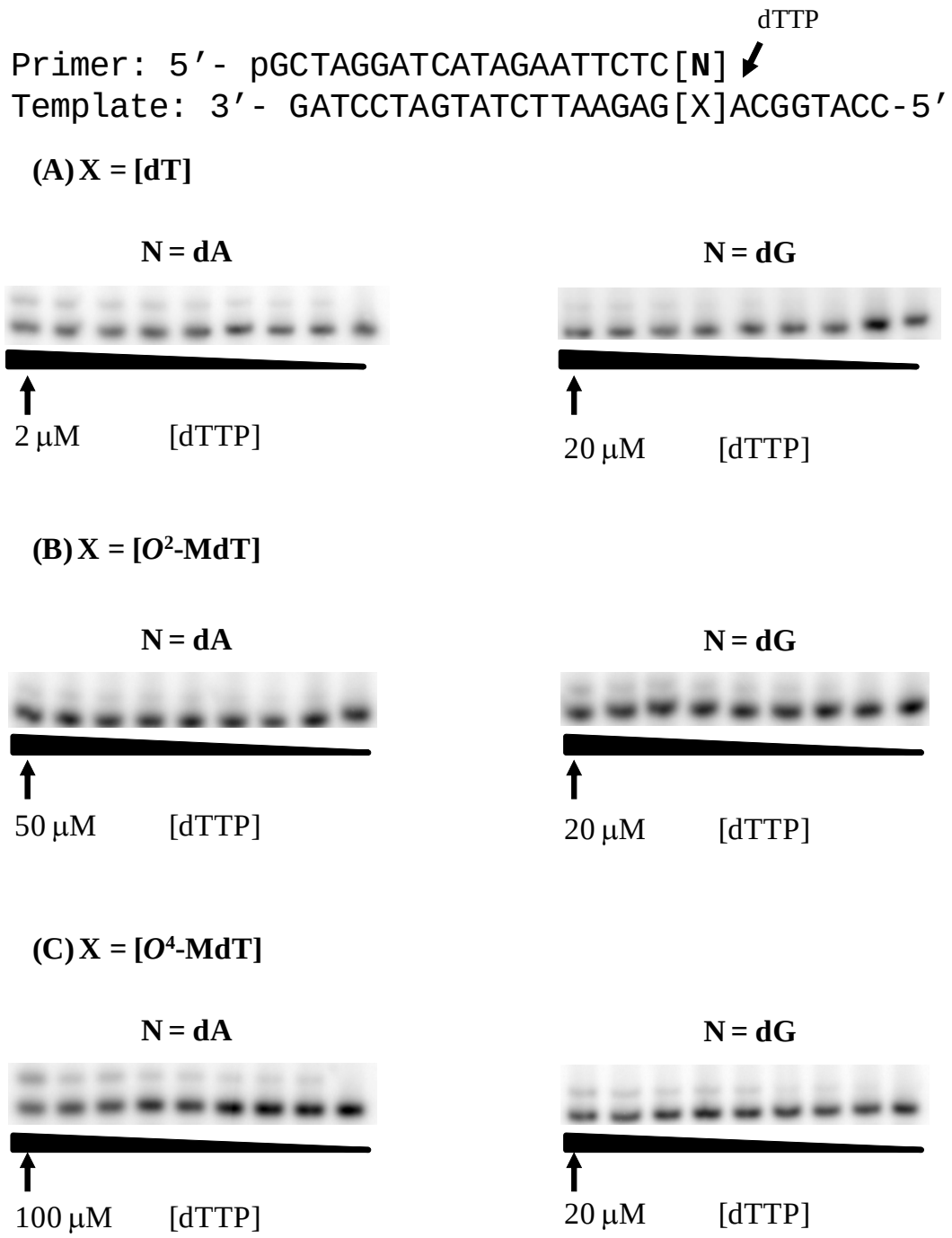
dTTP
Primer: 5′- pGCTAGGATCATAGAATTCTC[N]
Template: 3′- GATCCTAGTATCTTAAGAG[X]ACGGTACC-5′
(A) X = [dT]
N = dA
N = dG
2 μM [dTTP]
20 μM [dTTP]
(B) X = [O2-MdT]
N = dA
N = dG
50 μM [dTTP]
20 μM [dTTP]
(C) X = [O4-MdT]
N = dA
N = dG
100 μM [dTTP]
20 μM [dTTP]

Figure S15

Name	Sequence	O^4-MdT (low dNTPs)	O^4-MdT (6 hr)
		Yeast Polymerase η	
7mer	d(AATTCTC)	6	26
8mer	d(AATTCTCA)	3	3
8mer	d(AATTCTCG)	8	7
11A	d(AATTCTCATGC)	10	3
11G	d(AATTCTCGTGC)	73	62

Table S1.

dNTP	k_{cat} (min^{-1})	K_m (μM)	k_{cat}/K_m (mM^{-1} min^{-1})	f_{ext}
		Extension with dTTP		
dT:dATP	9.5 ± 0.4	0.56 ± 0.02	17	1
dT:dGTP	5.3 ± 0.1	2.2 ± 0.3	2.5	0.15
O^2-MdT:dATP	9.5 ± 0.4	7.8 ± 0.8	1.2	1
O^2-MdT:dGTP	13 ± 1	7.5 ± 0.5	1.7	1.4
O^4-MdT:dATP	10 ± 1	26 ± 2	0.38	1
O^4-MdT:dGTP	27 ± 2	11 ± 1	2	5.2

*The K_m and k_{cat} were average values based on three independent measurements

Table S2.